Large Changes in the CRAC Segment of gp41 of HIV Do Not Destroy Fusion Activity if the Segment Interacts with Cholesterol[†]

Sundaram A. Vishwanathan,[‡,§] Annick Thomas,[§,||] Robert Brasseur,[||] Raquel F. Epand,[⊥] Eric Hunter,[‡] and Richard M. Epand*[,⊥]

Emory Vaccine Research Center, Yerkes, Emory University, 954 Gatewood Road, Atlanta, Georgia 30329, Department of Biochemistry and Biomedical Sciences, McMaster University, 1200 Main Street West, Hamilton, Ontario L8N 3Z5, Canada, and Faculté Universitaire des Sciences Agronomiques de Gembloux Centre de Biophysique Moléculaire Numérique, Passage des Déportés, 2 5030 Gembloux, Belgium

Received August 6, 2008; Revised Manuscript Received September 16, 2008

ABSTRACT: The membrane-proximal external region (MPER) of the gp41 fusion protein of HIV is highly conserved among isolates of this virus and is considered a target for vaccine development. This region also appears to play a role in membrane fusion as well as localization of the virus to cholesterol-rich domains in membranes. The carboxyl terminus of MPER has the sequence LWYIK and appears to have an important role in cholesterol interactions. We have tested how amino acid substitutions that would affect the conformational flexibility of this segment could alter its interaction with cholesterol. We studied a family of peptides (all peptides as *N*-acetyl-peptide amides) with P, G, or A substituting for W and I of the LWYIK sequence. The peptide having the greatest effect on cholesterol distribution in membranes was the most flexible one, LGYGK. The corresponding mutation in gp41 resulted in a protein retaining 72% of the fusion activity of the wild-type protein. Two other peptides were synthesized, also containing two Gly residues, GWGIK and LWGIG, and did not have the ability to sequester cholesterol as efficiently as LGYGK did. Making the corresponding mutants of gp41 showed that these other two double Gly substitutions resulted in proteins that were much less fusogenic, although they were equally well expressed at the cell surface. The study demonstrates that drastic changes can be made in the LWYIK segment with the retention of a significant fraction of the fusogenic activity, as long as the mutant proteins interact with cholesterol.

The region of the ectodomain of gp41 from HIV adjacent to the transmembrane segment has been termed the membrane-proximal external region (MPER).[1] The MPER is rich in Trp residues and is highly conserved among strains of HIV (Figure 1). This segment has been shown to have an important contribution to fusogenic potency (*1*−*5*). In addition, a synthetic peptide corresponding to this domain has membrane destabilizing properties (*6, 7*). The presence of the raft-component lipids sphingomyelin and cholesterol is important for this peptide to be able to destabilize membranes (*8, 9*). The neutralizing antibody, 4E10, recognizes the MPER domain specifically when it associates with rafts and blocks membrane fusion (*4, 5, 10*).

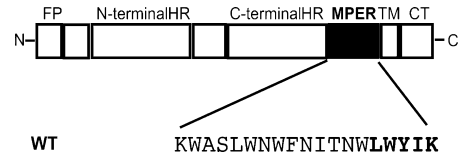

FIGURE 1: Schematic representation of HIV-1 gp41. The sequence of MPER is shown with the C-terminal CRAC segment, LWYIK, highlighted. MPER lies between the C-terminal heptad repeat (HR) and the transmembrane (TM) region. FP, fusion peptide; CT, cytoplasmic tail.

One of the features that connect MPER to raft domains is the presence of the carboxyl-terminal segment of MPER, LWYIK. This segment, when fused to the maltose binding protein, was able to bind to cholesteryl-hemisuccinate agarose (*11*). In addition, *N*-acetyl-LWYIK-amide has been shown to sequester cholesterol to membrane domains and to insert more deeply into membranes in the presence of cholesterol (*12*). The requirements for a CRAC domain have been established through analysis of the sequences of several proteins that interact with cholesterol. These proteins were

[†] This work was supported by the Canadian Natural Sciences and Engineering Research Council (Grant RGPIN9848-08) and "Ministère de la Région Wallonne" Contract n°14540 (PROTMEM). We also thank the "FRSM" (Contract n°3.4505.02) for financial support. The work on mutagenesis and HIV-1 fusion was supported by Grant R01 AI-33319 from the National Institutes of Health. R.B. is Research Director at the National Funds for Scientific Research of Belgium (FNRS). A.T. is Research Director at the "Institut National de la Santé et de la Recherche Médicale" (INSERM France).

* To whom correspondence should be addressed. Telephone: (905) 525-9140, ext. 22073. Fax: (905) 521-1397. E-mail: epand@mcmaster.ca.

[‡] Emory University.

[§] These authors contributed equally to the work.

[||] Faculté Universitaire des Sciences Agronomiques de Gembloux Centre de Biophysique Moléculaire Numérique.

[⊥] McMaster University.

[1] Abbreviations: MPER, membrane-proximal external region; CRAC, cholesterol recognition/interaction amino acid consensus; HIV, human immunodeficiency virus; PC, phosphatidylcholine; SOPC, 1-stearoyl-2-oleoylphosphatidylcholine; DSC, differential scanning calorimetry; T_m, phase transition temperature; ΔH, calorimetric enthalpy; MFP, mean force potential; MFI, mean fluorescence intensity; rmsd, root mean square deviation.

10.1021/bi8014828 CCC: $40.75 © 2008 American Chemical Society
Published on Web 10/21/2008

all found to possess the sequence pattern -L/V-$(X)_{(1-5)}$-Y-$(X)_{(1-5)}$-R/K-, in which $(X)_{(1-5)}$ represents one to five residues of any amino acid (*13*). Thus, the segment LWYIK is a CRAC domain. The fact that LWYIK fulfills the requirements of a CRAC domain may explain its ability to interact with cholesterol. Supporting the suggestion that the CRAC domain, LWYIK, of gp41 is responsible for interaction with cholesterol is our finding that the related sequence IWYIK destroys both the CRAC domain and cholesterol interactions (*14*). In addition, the presence of the CRAC domain, LWYIK, appears to facilitate membrane fusion in cells. The L679I mutant, i.e., a single conservative mutation that destroys both the CRAC domain and cholesterol sequestration, also caused a marked decrease in the level of fusion of cells expressing the mutant gp41 (*14*).

The reason LWYIK preferentially interacts with cholesterol compared with several non-CRAC peptide sequences has been suggested to involve their structural flexibility, their position at the interface, and their noncovalent bonding with cholesterol. LWYIK, as part of an MPER segment peptide, is found embedded in the membrane (*15*). This may also result in it being less available for immune surveillance. The LWYIK segment has also been found to be more hydrophobic (*16*) and to insert more deeply into the membrane than the less active IWYIK segment (*16, 17*). In this work, we systematically alter the conformational flexibility of LWYIK by substituting and testing all of the possible sequences containing either G, A, or P substituted for W and I in LWYIK. Residues W and I are not required to maintain the CRAC motif. All peptides studied for their interactions with lipids were all in the form of *N*-acetyl-peptide-amides. Peptide sequences should be assumed to be in this form even when not specifically indicated. Among this family of nine peptides, the most active in sequestering cholesterol was LGYGK, demonstrating as had been suggested by in silico calculations that conformational flexibility was a factor favoring interaction with cholesterol (*14*). We also compared this peptide with two others having substitutions with two additional Gly residues, i.e., GWGIK and LWGIG. These latter two peptides do not have CRAC sequences and are therefore less likely to interact with cholesterol.

We also examined the effects of mutations in the LWYIK pentapeptide in the context of the entire HIV-1 Env protein, gp41, by assessing the ability of the mutated protein to promote cell−cell fusion. This allowed us to correlate changes in the cholesterol sequestering ability of the peptide with its role in fusion when incorporated into the intact protein. We demonstrate that despite the high degree of conservation of the LWYIK segment, the drastically modified mutant W680G/I682G still retains considerable fusogenic activity. Another gp41 mutated in this pentapeptide that has been reported to have considerable fusogenic activity even though it no longer has a CRAC segment is the Y681P mutant (*18*). Recently, the amino-terminal portion of MPER has been substituted with a membrane-perturbing peptide, indolicidin, with partial retention of fusion activity (*19*). This study compares the retention of fusion activity with the ability of the C-terminal portion of MPER to sequester cholesterol.

MATERIALS AND METHODS

Materials. The peptides are all synthesized as *N*-acetyl-peptide-amides, i.e., blocked at the terminal amino and carboxyl groups. Peptides GWGIK and LWGIG were synthesized by Synbiosci Corp. (Livermore, CA) and purified by HPLC to >95% purity. Peptides LPYPK, LAYPK, LGYPK, LPYAK, LGYAK, LAYAK, LGYGK, LPYGK, and LAYGK were synthesized by GL Biochem (Shanghai, China) and purified by HPLC to >95% purity. Phospholipids and cholesterol were purchased from Avanti Polar Lipids (Alabaster, AL).

Preparation of Samples for DSC. Phospholipid and cholesterol were codissolved in a chloroform/methanol mixture (2/1, v/v). For samples containing peptide, an aliquot of a solution of the peptide in methanol was added to the lipid solution in a chloroform/methanol mixture. The solvent was then evaporated under a stream of nitrogen with constant rotation of a test tube to deposit a uniform film over the bottom third of the tube. The last traces of solvent were removed by placing the tube under high vacuum for at least 3 h. The lipid film was then hydrated with 20 mM PIPES, 1 mM EDTA, and 150 mM NaCl with 0.002% NaN_3 (pH 7.40) and suspended by intermittent vortexing and heating to 50 °C over a period of 2 min under argon.

Differential Scanning Calorimetry (DSC). Measurements were taken using a Nano differential scanning calorimeter (Calorimetry Sciences Corp., Lindon, UT). Each sample was scanned with two or three cycles of heating and cooling between 0 and 60 °C. The scan rate was 2 °C/min, and there was a delay of 5 min between sequential scans in a series to allow for thermal equilibration. The features of the design of this instrument have been described previously (*20*). DSC curves were analyzed by using the fitting program, DA-2, provided by Microcal Inc. (Northampton, MA) and plotted with Origin, version 5.0.

Membrane Partitioning Studies. Subsequent to DSC analysis, samples were transferred to 1 mL silanized polycarbonate tubes and centrifuged at 200000*g* (100000 rpm) for 150 min at 25 °C in a Sorvall RC M120 centrifuge. A clear supernatant was collected in silanized glass tubes, and the spectra were recorded between 350 and 250 nm using a Cary 50Bio spectrophotometer. The supernatant from a suspension of lipid without peptide was used as a blank. The absorbance at 280 nm, corrected for the blank and for light scattering, was used to calculate the amount of peptide remaining in the supernatant, compared with the total concentration of peptide determined by absorbance before the addition of lipid.

Modeling: Structure Properties. A search for the most favorable conformation of each of the peptides was conducted using PepLook (*21*). The energy of peptide conformations is calculated by an all-atom description of structures with the addition of van der Waals, electrostatic, internal, and external hydrophobicity energy terms. The van der Waals contribution was calculated using the 6-12 Lennard-Jones description of the energy of interactions between unbonded atoms (*22*). Coulomb's equation was used for electrostatic interactions between unbonded charged atoms with a dielectric "constant" sigmoidally varying from 1 to 80 for the region between atoms and using FCPAC partial atomic charges (*23*). The intramolecular hydrophobicity contribution

to stability was calculated using atomic Etr (energy of transfer) and the fractions of atomic surface covered by the atoms in interactions. Seven atomic types are used for calculating Etr (*24*). When structures are calculated in water, an external hydrophobicity energy term where the solvent-accessible surface of atoms is calculated by the method of Shrake and Rupley with 162 points accounts for the contribution of solvent (*25*−*27*). From the 500000 calculated models, the 99 most stable in most instances or the 999 most stable in some cases are sorted. The energy of each model is calculated as the sum of the van der Waals and electrostatic terms. Calculations were carried out under conditions of implicit water, lipids, and membrane interface.

Cell−*Cell Fusion: (i) Cell Culture.* 293T or African green monkey kidney COS-1 cells and TZM-BL cells were used for fusion assays. TZM-BL HeLa-based HIV-1 indicator cells (*28*) that show a high susceptibility to HIV-1 infection were kindly provided by Tranzyme Inc. (Birmingham, AL). These cells contain reporter genes, luciferase and β-galactosidase, that are expressed in the presence of Tat, under the influence of HIV-1 LTR. Cells were subcultured every 3−4 days by trypsinization and maintained in Dulbecco's modified Eagle's medium (DMEM) supplemented with 10% fetal bovine serum and antibiotics.

(ii) Mutagenesis and Plasmid Vectors. Mutations of the HIV-1 membrane-proximal external region (MPER) were designed by QuikChange (Stratagene, La Jolla, CA), using an NL4.3 (laboratory-adapted X4 strain) KpnI−BamHI envelope fragment that was cloned into vector pSP72. The mutated envelope fragment was subsequently subcloned into an SV-40-based vector (pSRHS) that expresses Tat and Env (*1*). Subsequently, the mutated envelope was introduced into envelope expression vector pCDNA3.1/V5-His-TOPO following the manufacturer's instructions (Invitrogen, Carlsbad, CA), and employed for Env surface expression studies. All mutations were confirmed by sequencing.

(iii) Cell−*Cell Fusion Assays.* 293T or COS-1 cells were transfected with pCDNA or pSRHS constructs expressing wild-type and mutant HIV-1 envelopes using Fugene 6 transfection reagent (Roche Diagnostics Corp., Indianapolis, IN). The transfected cells expressing the WT or mutant Env were mixed with TZM-BL cells (1/5 ratio) 20−24 h post-transfection, and replated in 24-well plates. After 20 h, cell−cell fusion was assessed by measuring luciferase activity (Luciferase Assay System, Promega) according to the manufacturer's protocol.

(iv) Cell Surface Expression of Env Proteins. Thirty-six to forty hours after transfection of the 293T cells with the pCDNA3.1 vectors encoding WT and mutant Envs, the cells were trypsinized and washed in flow cytometry buffer (PBS with 0.1% BSA and 0.1% NaN_3). The Env molecules on the surface of the 293T cells were fluorescently labeled by incubating 100 μL of harvested 293T cells with 0.5 μg/mL gp120-specific b12 (a gift from D. Burton, Scripps Research Institute, La Jolla, CA) at room temperature for 1 h. This antibody had been tagged with Alexa Fluor647 (Invitrogen) according to the manufacturer's instructions. The cell surface expression of Env was evaluated by flow cytometry with FACSCalibur (Becton Dickinson, Franklin Lakes, NJ); the data were analyzed using FloJo version 8.2 (Tree Star Inc., Ashland, OR), and the mean fluorescence intensity (MFI) was calculated from the acquisition of at least 30000 gated events. Nonspecific background fluorescence due to the secondary antibody was subtracted from the MFIs.

RESULTS

DSC. DSC can be used to assess the effect of peptides on the miscibility of cholesterol and SOPC (*29*). We have used this method to demonstrate that IWYIK is less able to sequester cholesterol than LWYIK (*14*) and that the peptides AWYIK and VWYIK had intermediate potencies (*30*). In this work, we compare the effects of several modified versions of LWYIK at 5, 10, or 15 mol % on the phase transition behavior of SOPC alone or in the presence of 30 or 40 mol % cholesterol.

The phase transition of SOPC in the absence of cholesterol was at 5 °C in cooling scans, with an enthalpy of 4 kcal/mol. Addition of any of the peptides studied in this work, except for LWGIG, at 5, 10, or 15 mol % had no effect on the transition temperature or enthalpy of pure SOPC. The transition temperature of pure SOPC was affected only by the peptide LWGIG that caused a shift to 4.7, 4.7, and 4.5 °C at 5, 10, and 15 mol % peptide, respectfully. We suggest this is a consequence of the lack of charge on this peptide. After centrifugation of the mixtures of SOPC with the peptides at 5, 10, or 15%, all the peptides were found in the supernatant except for LGYPK for which ~40% of the peptide was bound to the lipid.

DSC curves of a few representative peptides in the presence of SOPC with 30% cholesterol are shown in Figure 2. We compare the effects of the most flexible peptide, LGYGK (top row of Figure 2), with those of the least flexible in the series, LPYPK (middle row of Figure 2), and a non-CRAC peptide, GWGIK (bottom row of Figure 2). There is a large difference in the DSC profile for the scans with LGYGK that have qualitatively larger peaks than those with the least flexible peptide, LPYPK. The shapes of the curves for LGYGK are similar to those of the wild-type sequence LWYIK that have been previously published (*12*). By comparison, the curves at low mole fractions of GWGIK exhibit a broader transition, indicating a less pure SOPC-enriched domain. Differences are also observed when comparing the enthalpy of SOPC with 30 or 40% cholesterol in the presence or absence of the various peptides (Table 1). The precision of the enthalpy values is ±10%. However, the accuracy is estimated to be ±15% for the SOPC mixtures with 30% cholesterol and ±25% for the SOPC mixtures with 40% cholesterol. This is a result of inaccuracies in drawing the baseline on the low-temperature side of the transition and is somewhat larger for higher cholesterol mole fractions because of the greater broadness of the transitions. The only peptide not included in this table is LWGIG because it caused a lowering of the transition temperature in these mixtures that did not allow measurement of the full transition peak on cooling. For the remainder of the peptides, there is some similarity in their behavior, since they all generally exhibit transitions for SOPC that are larger than that of the pure lipid. This is confirmed with the SOPC mixture with 40% cholesterol. However, the differences among the peptides are more clearly revealed in the results from the SOPC mixture with 30% cholesterol (Table 1). For example, peptides with P in the fourth position, including LPYPK, LAYPK, and LGYPK, have enthalpies of <1 kcal/mol for all three

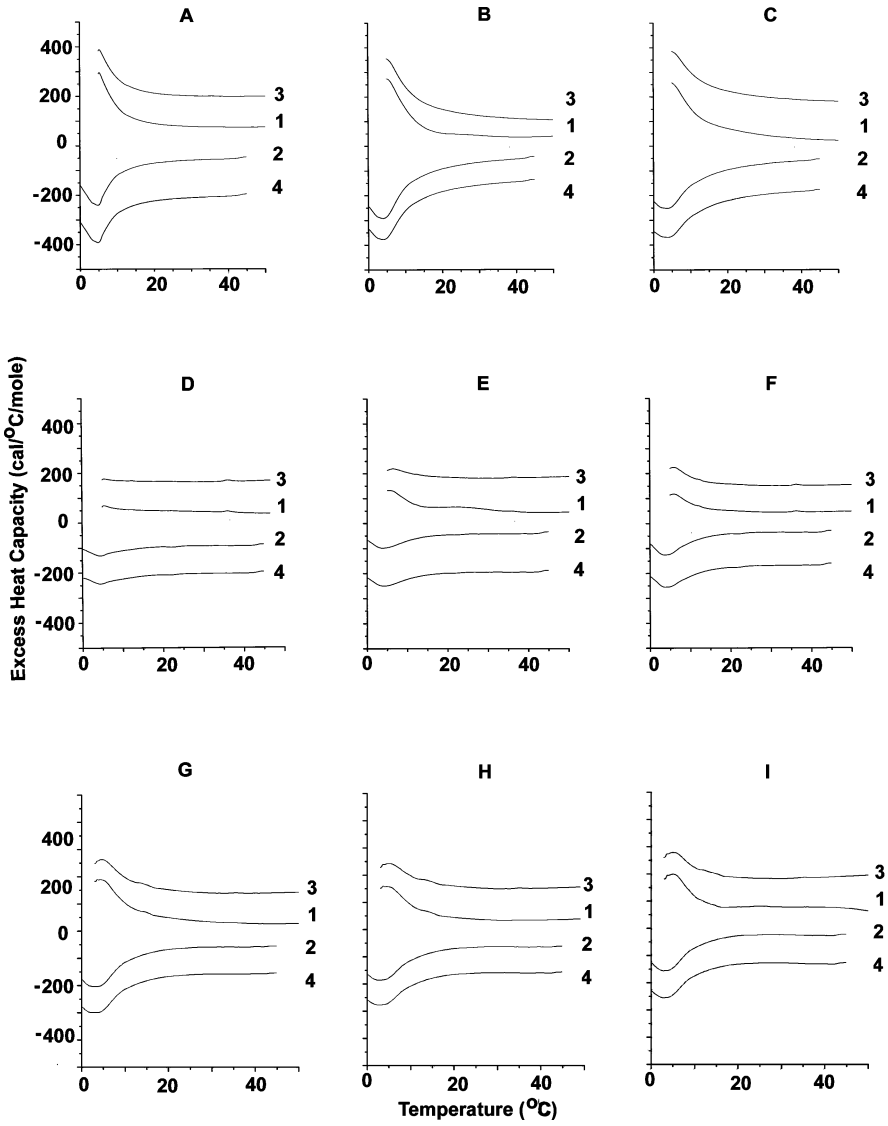

FIGURE 2: Differential scanning calorimetry of SOPC with 30 mol% cholesterol. The scan rate was 2 K/min. The lipid concentration was 2.5 mg/mL in 20 mM PIPES, 1 mM EDTA, 150 mM NaCl, and 0.002% NaN_3 (pH 7.40). Sequential heating and cooling scans between 0 and 50 °C. Numbers are the order in which the scans were carried out, with scans 1 and 3 being heating scans, each of which was followed by one of the cooling scans (2 or 4). Scans were displaced along the *y*-axis for clarity of presentation. *N*-Acetyl-LGYGK-amide is added to samples whose DSC is shown in panels A−C, *N*-acetyl-LPYPK-amide in panels D−F, and *N*-acetyl-GWGIK-amide in panels G−I. The peptide content is 5 mol % for panels A, D, and G, 10 mol % for panels B, E, and H, and 15 mol % for panels C, F, and I.

concentrations of peptide (with the small exception of LPYPK at 15%, which is just greater than 1). The non-CRAC peptide, GWGIK, also has enthalpies of <1 kcal/mol with this lipid mixture. In comparison the wild-type peptide, LWYIK and LGYGK have enthalpies of ≥1 kcal/mol for all three peptide concentrations. In particular, at 5 mol % LGYGK is the peptide that exhibits the highest enthalpy for the SOPC transition in the mixture with 30% cholesterol, and in the 40% cholesterol mixture, it gives an SOPC peak that has a larger enthalpy than that for the wild type, LWYIK. Curiously, GWGIK produces the largest peaks for the SOPC transition in mixtures with 40% cholesterol, with magnitudes comparable to those observed with 30% cholesterol and little dependence on peptide concentration. It is clear that GWGIK behaves differently with these lipid mixtures than do the other peptides.

Another consequence of the formation of cholesterol-rich domains can be that the sterol passes its solubility limit in a region of the membrane, forming crystallites. Anhydrous crystalline cholesterol is known to undergo a crystalline polymorphic phase transition at 38 °C when heated and at 23 °C when cooled at a scan rate of 2 °C/min (*31*), with an enthalpy of 910 cal/mol (*32*). This hysteresis is characteristic of anhydrous cholesterol crystals and provides a criterion for identifying the presence of these crystals. There are no cholesterol crystals found in the absence of peptide, even up to an SOPC/cholesterol ratio of 1/1. At SOPC/cholesterol molar ratios of 7/3 and 6/4, most of the peptides induce the formation of cholesterol crystals corresponding to ∼4, ∼5, or ∼10% of the total amount of cholesterol at 5, 10, and 15% peptide, respectively. The polymorphic transition of anhydrous cholesterol crystallites can be just discerned for LPYPK in Figure 2. It is also evident in scans with LGYGK using 40% cholesterol in SOPC (not shown). The only peptide that does not exhibit cholesterol crystallites is LWGIG, which shows no formation of anhydrous cholesterol crystals at any of the SOPC/cholesterol ratios. It was mentioned above that LWGIG was the only peptide to affect

Table 1: Enthalpies of the Chain Melting Transition of SOPC

mol % peptide	peptide	ΔH (kcal/mol) 7/3 SOPC/cholesterol	ΔH (kcal/mol) 6/4 SOPC/cholesterol
0	none	0.52	0.1
5	LWYIK	1.0	0.1
10		1.1	0.3
15		1.4	0.5
5	LPYPK	0.4	0.2
10		0.5	0.3
15		1.1	0.4
5	LAYAK	0.4	0.3
10		0.6	0.6
15		1.0	0.5
5	LGYGK	1.5	0.2
10		1.4	0.3
15		1.2	0.3
5	LPYAK	1.1	0.3
10		1.4	0.3
15		1.1	0.4
5	LAYPK	0.5	0.3
10		0.6	0.4
15		0.9	0.4
5	LPYGK	0.8	0.2
10		1.5	0.3
15		1.3	0.4
5	LGYPK	0.6	0.3
10		0.3	0.4
15		0.8	0.4
5	LAYGK	0.9	0.2
10		1.0	0.2
15		1.0	0.3
5	LGYAK	0.7	0.2
10		0.5	0.2
15		0.8	0.1
5	GWGIK	0.9	0.5
10		0.8	0.7
15		0.7	0.9

the transition of pure SOPC. This combined with the lack of formation of cholesterol crystallites suggests that this peptide does not preferentially interact with either cholesterol or SOPC in mixtures of the two lipids. In addition, peptide GWGIK shows no formation of cholesterol crystals at a 6/4 SOPC/cholesterol ratio, also suggesting that there may be only a weak preferential interaction of this peptide with one of these two lipids. However, there is a small peak corresponding to cholesterol crystals in the mixtures of this peptide with 30% cholesterol (Figure 2). This is another indication of the unusual behavior of the interaction of this peptide with SOPC/cholesterol mixtures. Thus, the two non-CRAC peptides have the weakest tendency to preferentially interact with cholesterol. It should be pointed out, however, that cholesterol crystals could form if the peptide preferentially interacted with the SOPC component, resulting in cholesterol being removed from this domain. Hence, we do not consider the formation of cholesterol crystallites as good evidence for preferential binding of peptides to cholesterol. However, the converse is true, i.e., that the lack of cholesterol crystallite formation is useful as an indication of the lack of preferential interaction of the peptide with cholesterol.

For all three mixtures of SOPC in the presence of cholesterol, almost all of the peptides were found bound to the lipid pellet after centrifugation. This indicates that differences in membrane partitioning among the peptides that were studied had only a minor effect on their ability to affect the phase transitions of the lipid mixtures. It also shows that

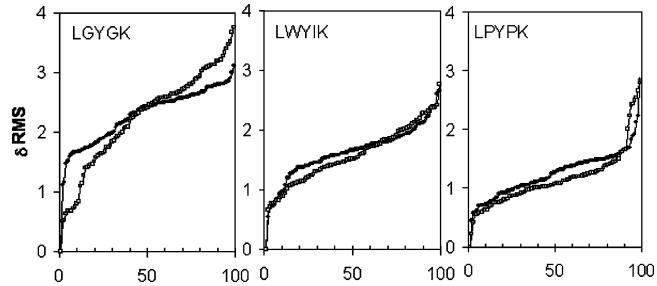

FIGURE 3: rmsd variation of the LWYIK, LGYGK, and LPYPK models calculated with PepLook (*21*). Models are calculated under hydrophobic (□) and hydrophilic (●) conditions. At the end of the iterative PepLook process, 99 models of lower energy were sorted. They are plotted by their variation in rms by reference to the structure of the Prime.

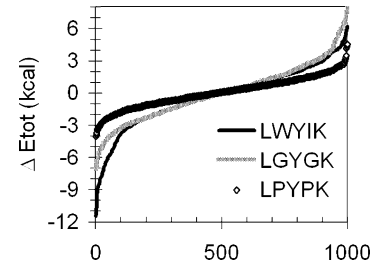

FIGURE 4: Energy variation of the models of LWYIK, LGYGK, and LPYPK calculated by PepLook (*21*). At the end of the iterative calculation process, 999 models instead of 99 models of lower energy were sorted. They are plotted by their variation in energy by reference to the 500th model of the population. Energies are sums of van der Waals and electrostatic contributions.

cholesterol increases the degree of partitioning of these peptides to the membrane compared with pure SOPC.

Modeling: Three-Dimensional Structures of the Peptides Were Calculated under Conditions of Hydrophilic, Interfacial, and Hydrophobic Media. We used PepLook to calculate the peptide structural possibilities (Figure 3). Analyses of the root-mean-square deviation (rmsd) of the 99 PepLook models demonstrate that the LGYGK peptide has the largest plasticity with a rmsd of up to 4 Å, the most constrained peptide being LPYPK. When we sort the 999 PepLook models of lower energy at the membrane interface and rank them by ΔE (Figure 4), we notice that LWYIK has a wider energy distribution than LPYPK. Therefore, LPYPK is both structurally and energetically restricted; LGYGK has wider structural and energy possibilities, and LWYIK with intermediate structural possibilities has the best capacity for energy stabilization. This demonstrates that LWYIK is the peptide that shows the greatest stability at a membrane interface.

Studies in the Context of HIV-1 Env: (i) Mutagenesis of the Membrane-Proximal External Region (MPER) of HIV-1 gp41. We examined the effects of mutations in the LWYIK segment in the context of the entire HIV-1 Env. This peptide is part of the HIV-1 MPER in the gp41 ectodomain whose crucial role in viral fusion has been established (*1*). We employed the QuikChange mutagenesis method to generate mutants in which two glycine residues were substituted in the LWYIK segment of MPER. The following mutants were created (sequences in parentheses show the modified form of the LWYIK segment that was generated and are how these mutants will be mentioned below): L679G/Y681G (GWGIK), Y681G/K683G (LWGIG), and W680G/I682G (LGYGK).

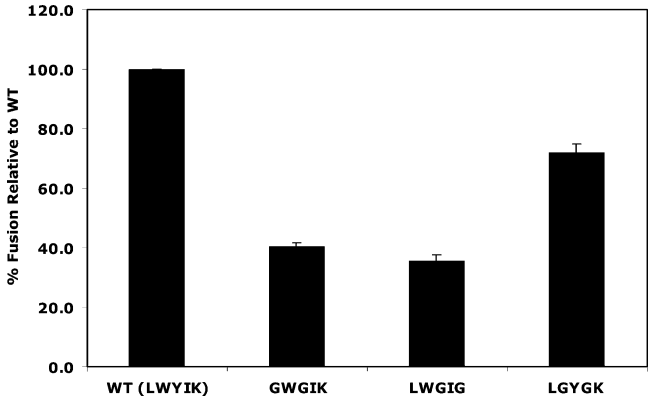

FIGURE 5: Cell−cell fusion assays of wild-type (WT) and MPER mutants GWGIK, LWGIG, and LGYGK. Data are averages of four experiments (with transfected COS-1 cells), for each of the samples which were run in duplicate. Luciferase activity was determined by following the manufacturer's instructions and normalized as a percentage of that observed with the wild type.

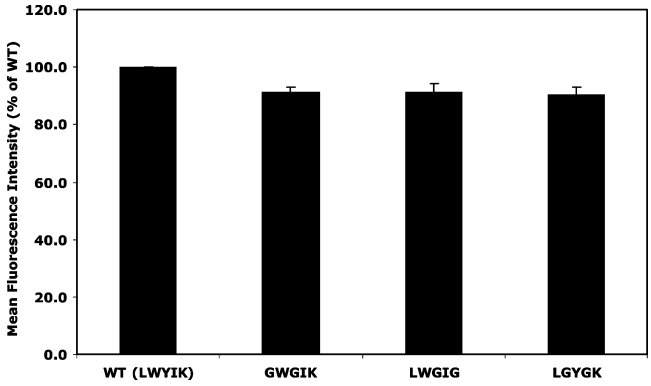

FIGURE 6: Cell surface expression (measured by calculating the mean fluorescence intensity, MFI) of mutant and WT Env proteins. The results indicate the expression of mutant Env on the surface of 293T cells as a percentage of WT.

(ii) Effects on Cell−Cell Fusion. The fusion efficiency of LGYGK was somewhat lower than that of the wild type but was much greater than for LWGIG or GWGIK (Figure 5).

(iii) Cell Surface Expression of Env Proteins. There is only a small reduction of ~10% in the level of cell surface expression of any of the mutants, relative to the wild-type protein taken to be 100% (Figure 6).

DISCUSSION

We have shown previously that peptide LWYIK promoted the segregation of membrane lipids into cholesterol-rich and cholesterol-poor domains. Evidence of the formation of a domain depleted of cholesterol came from DSC, which exhibited a more cooperative and higher enthalpy gel to liquid crystalline phospholipid phase transition. Apparently, the other regions of the membrane that are enriched in cholesterol have a sufficiently high cholesterol concentration that they pass the solubility limit of cholesterol in the membrane, forming cholesterol crystallites (*12*). In addition, the presence of cholesterol was shown to allow a greater depth of penetration of LWYIK into the membrane bilayer (*17*). In this study, we introduced amino acid substitutions that would be expected to drastically alter the conformational flexibility of LWYIK. Gly has the smallest side chain and is expected to allow the greatest amount of conformational flexibility, while Pro is the most conformationally restricted because of its ring structure and Ala of intermediate flexibility.

LWYIK represents a CRAC sequence (*13*). According to the CRAC algorithm, the second and fourth residues of LWYIK can be substituted with any amino acid while maintaining the peptide as a CRAC sequence. We studied a series of peptides with the W and I residues substituted with A, P, or G. Hence, all of the modified sequences correspond to CRAC segments. In addition, we studied GWGIK and LWGIG that also have two amino acid substitutions in LWYIK, but these two peptides are not CRAC sequences. We find that all of the CRAC sequences and even GWGIK induce an increased enthalpy of the SOPC transition in mixtures of SOPC and cholesterol (Table 1). However, the non-CRAC sequences GWGIK and LWGIG behave differently. LWGIG is the only peptide of the series to affect the phase transition of pure SOPC. In addition, this peptide has the greatest effect in lowering the temperature of the transition of mixtures of SOPC with cholesterol. Furthermore, LWGIG is the only peptide that does not promote the formation of cholesterol crystals in mixtures of SOPC with either 30 or 40% cholesterol. GWGIK also has unique properties. It exhibits the highest transition enthalpy with mixtures of SOPC and 40% cholesterol, but these enthalpies are similar to those observed with this peptide in mixtures containing 30% cholesterol. Unlike the case for wild-type LWYIK, there is no increase in the enthalpy of this transition with an increase in peptide concentration. In addition, GWGIK induces the formation of cholesterol crystallites with mixtures of SOPC and 30% cholesterol, but curiously not with 40% cholesterol. These non-CRAC peptides have behavior qualitatively different from that of the others.

Among the CRAC peptides, the one that induces a somewhat greater enthalpy for the SOPC transition (Table 1) is the sequence LGYGK. We have therefore introduced these two amino acid substitutions into the LWYIK segment of the intact Env protein by substituting W^{680} and I^{682} with G. We find that expression of the resultant mutant protein supports 72% of the fusion activity of the WT protein (Figure 5). It is remarkable that two such nonconservative substitutions could be introduced into an invariant region of HIV-1 gp41, with only a relatively modest lost of fusion activity. It has recently been demonstrated that a large segment of the MPER region can be replaced with a sequence of amino acids corresponding to a membrane-perturbing peptide (*19*). The more active mutants retained the segment WYIK and had only partial fusogenic activity. It remains to be determined how important the LWYIK segment is for full fusion activity and for cholesterol recognition in these constructs. The finding that peptide LGYGK retained considerable activity in segregating cholesterol in model membranes combined with the observation that introduction of this sequence in the intact gp41 protein allowed considerable retention of fusogenic activity is good evidence that there is a correlation between the ability of this region of the protein to be sequestered to a cholesterol-rich region and its infectivity.

Thus, when one compares mutants with similar kinds of substitutions, such as I^{679}, V^{679}, and A^{679}, or for the group of three mutants described here with the substitution of two Gly residues, there is good correlation between reorganization

of cholesterol in model membranes by the corresponding peptide and the fusogenicity of the virus. However, the interaction with cholesterol is not the only factor determining the fusogenic activity of the mutant forms of gp41. Thus, the L679I mutant has approximately the same fusogenic activity that the W680G/I682G mutant does. Nevertheless, peptide LGYGK is much more effective in sequestering cholesterol (Table 1) than is peptide IWYIK (*30*). This supports the CRAC hypothesis for cholesterol interactions since LGYGK is a CRAC sequence but IWYIK is not. Although LGYGK has a stronger interaction with cholesterol than IWYIK, the L679I and W680G/I682G gp41 mutants have comparable fusogenic activity. Changing L to I involves only moving a methyl group from one carbon atom to another, while the W680G/I682G mutant replaces two hydrophobic, bulky residues with two that are small, conformationally flexible, and not hydrophobic in a region of gp41 that is invariant. There are likely other factors, in addition to the interaction with cholesterol that will determine the biological properties of these mutants. Nevertheless, within a similar series of mutations, the correlation between the peptide affecting cholesterol distribution and the fusogenic activity of the mutant gp41 is good. In addition, the fact that we can make a drastic change in the LWYIK segment of gp41, and still retain considerable fusogenic activity as well as cholesterol sequestering ability (with the W680G/I682G mutant), is good evidence that interactions of this region of the protein with cholesterol play an important but not unique role in viral fusion.

An indication that cholesterol is important for the membrane interactions of HIV is the finding that the cholesterol/phospholipid ratios in the viral membrane of HIV are generally higher than that of the host membranes (*33*), although the exact increase varies from strain to strain and also depends on other factors, including the growth conditions and the type of target cell used. It has been suggested that the HIV envelope has a lipid composition suggesting that it has raftlike properties (*34*). HIV viral membrane proteins have also been shown to be sequestered into cholesterol-rich raft domains in the membrane during viral assembly (*35*). Cell membrane raft domains are important for viral entry and assembly (*36*). Cholesterol may be particularly important for viral fusion and internalization since these processes are inhibited by lower levels of viral membrane cholesterol even though membrane binding is not inhibited (*37*). Similar to cholesterol depletion, mutations in the MPER region that would be expected to reduce cholesterol affinity lead to a reduced level of fusion. The presence of the CRAC segment will allow the virus to sequester itself into specific host cholesterol domains and bud out of the cell, presumably containing an optimal amount of cholesterol in its own membrane.

It is also interesting to consider how cholesterol could affect the interaction of the intact HIV with membranes since there has been some imaging of the native structure of Env on the surface of the virion. One study proposed a splayed-legs model for Env in which the Env trimer positions itself in the viral membrane like a tripod (*38*). This model suggests extensive interaction of gp41 molecules with the viral membrane and possible interaction of the Env with the cholesterol-rich membrane domain on the target cell membrane. This could affect Env stability and subsequent internalization. However, there is an alternate model (*39*) in which a compact stalklike Env structure interacts with membranes. In this model, there is less interaction of gp41 monomers with the membrane, more with each other. For this model, it is difficult to visualize the possible effects of modifications of the CRAC segment on viral entry.

Our results indicate that the CRAC domain is important for gp41-induced cell−cell fusion. Its importance in virus−cell fusion is uncertain. On the basis of the model presented in ref *38*, it would be likely that this lipid interaction also has a role in virus−cell fusion.

REFERENCES

1. Salzwedel, K., West, J. T., and Hunter, E. (1999) A conserved tryptophan-rich motif in the membrane-proximal region of the human immunodeficiency virus type 1 gp41 ectodomain is important for Env-mediated fusion and virus infectivity. *J. Virol. 73*, 2469–2480.
2. Munoz-Barroso, I., Salzwedel, K., Hunter, E., and Blumenthal, R. (1999) Role of the membrane-proximal domain in the initial stages of human immunodeficiency virus type 1 envelope glycoprotein-mediated membrane fusion. *J. Virol. 73*, 6089–6092.
3. Dimitrov, A. S., Rawat, S. S., Jiang, S., and Blumenthal, R. (2003) Role of the fusion peptide and membrane-proximal domain in HIV-1 envelope glycoprotein-mediated membrane fusion. *Biochemistry 42*, 14150–14158.
4. Huarte, N., Lorizate, M., Maeso, R., Kunert, R., Arranz, R., Valpuesta, J. M., and Nieva, J. L. (2008) The broadly neutralizing anti-HIV-1 4E10 monoclonal antibody is better adapted to membrane-bound epitope recognition and blocking than 2F5. *J. Virol. 82*, 8986–8996.
5. Lorizate, M., Huarte, N., Saez-Cirion, A., and Nieva, J. L. (2008) Interfacial pre-transmembrane domains in viral proteins promoting membrane fusion and fission. *Biochim. Biophys. Acta 1778*, 1624–1639.
6. Suarez, T., Gallaher, W. R., Agirre, A., Goni, F. M., and Nieva, J. L. (2000) Membrane interface-interacting sequences within the ectodomain of the human immunodeficiency virus type 1 envelope glycoprotein: Putative role during viral fusion. *J. Virol. 74*, 8038–8047.
7. Suarez, T., Nir, S., Goni, F. M., Saez-Cirion, A., and Nieva, J. L. (2000) The pre-transmembrane region of the human immunodeficiency virus type-1 glycoprotein: A novel fusogenic sequence. *FEBS Lett. 477*, 145–149.
8. Saez-Cirion, A., Nir, S., Lorizate, M., Agirre, A., Cruz, A., Perez-Gil, J., and Nieva, J. L. (2002) Sphingomyelin and cholesterol promote HIV-1 gp41 pretransmembrane sequence surface aggregation and membrane restructuring. *J. Biol. Chem. 277*, 21776–21785.
9. Shnaper, S., Sackett, K., Gallo, S. A., Blumenthal, R., and Shai, Y. (2004) The C- and the N-terminal regions of glycoprotein 41 ectodomain fuse membranes enriched and not enriched with cholesterol, respectively. *J. Biol. Chem. 279*, 18526–18534.
10. Lorizate, M., Cruz, A., Huarte, N., Kunert, R., Perez-Gil, J., and Nieva, J. L. (2006) Recognition and Blocking of HIV-1 gp41 Pretransmembrane Sequence by Monoclonal 4E10 Antibody in a Raft-like Membrane Environment. *J. Biol. Chem. 281*, 39598–39606.
11. Vincent, N., Genin, C., and Malvoisin, E. (2002) Identification of a conserved domain of the HIV-1 transmembrane protein gp41 which interacts with cholesteryl groups. *Biochim. Biophys. Acta 1567*, 157–164.
12. Epand, R. M., Sayer, B. G., and Epand, R. F. (2003) Peptide-induced formation of cholesterol-rich domains. *Biochemistry 42*, 14677–14689.
13. Li, H., and Papadopoulos, V. (1998) Peripheral-type benzodiazepine receptor function in cholesterol transport. Identification of a putative cholesterol recognition/interaction amino acid sequence and consensus pattern. *Endocrinology 139*, 4991–4997.
14. Epand, R. F., Thomas, A., Brasseur, R., Vishwanathan, S. A., Hunter, E., and Epand, R. M. (2006) Juxtamembrane protein segments that contribute to recruitment of cholesterol into domains. *Biochemistry 45*, 6105–6114.
15. Sun, Z. Y., Oh, K. J., Kim, M., Yu, J., Brusic, V., Song, L., Qiao, Z., Wang, J. H., Wagner, G., and Reinherz, E. L. (2008) HIV-1

Broadly Neutralizing Antibody Extracts Its Epitope from a Kinked gp41 Ectodomain Region on the Viral Membrane. *Immunity 28*, 52–63.

16. Greenwood, A. I., Pan, J., Mills, T. T., Nagle, J. F., Epand, R. M., and Tristram-Nagle, S. (2008) CRAC motif peptide of the HIV-1 gp41 protein thins SOPC membranes and interacts with cholesterol. *Biochim. Biophys. Acta 1778*, 1120–1130.
17. Epand, R. M., Hughes, D. W., Sayer, B. G., Borochov, N., Bach, D., and Wachtel, E. (2003) Novel properties of cholesterol-dioleoylphosphatidylcholine mixtures. *Biochim. Biophys. Acta 1616*, 196–208.
18. Cao, J., Bergeron, L., Helseth, E., Thali, M., Repke, H., and Sodroski, J. (1993) Effects of amino acid changes in the extracellular domain of the human immunodeficiency virus type 1 gp41 envelope glycoprotein. *J. Virol. 67*, 2747–2755.
19. Vishwanathan, S. A., and Hunter, E. (2008) Importance of its Membrane-Perturbing Properties of the Membrane-Proximal External Region of Human Immunodeficiency Virus Type 1 gp41 to Viral Fusion. *J. Virol. 82*, 5118–5126.
20. Privalov, G., Kavina, V., Freire, E., and Privalov, P. L. (1995) Precise scanning calorimeter for studying thermal properties of biological macromolecules in dilute solution. *Anal. Biochem. 232*, 79–85.
21. Thomas, A., Deshayes, S., Decaffmeyer, M., Van Eyck, M. H., Charloteaux, B., and Brasseur, R. (2006) Prediction of peptide structure: How far are we? *Proteins 65*, 889–897.
22. Lins, L., Brasseur, R., De Pauw, M., Van Biervliet, J. P., Ruysschaert, J. M., Rosseneu, M., and Vanloo, B. (1995) Helix-helix interactions in reconstituted high-density lipoproteins. *Biochim. Biophys. Acta 1258*, 10–18.
23. Leach, A. R. (1996) van der Waals Interactions. In *Molecular Modelling: Principles and Applications* (Leach, A. R., Ed.) pp 171−177, Longman Ltd., Harlow, England.
24. Moult, J., and James, M. N. (1986) An algorithm for determining the conformation of polypeptide segments in proteins by systematic search. *Proteins 1*, 146–163.
25. Thomas, A., Milon, A., and Brasseur, R. (2004) Partial atomic charges of amino acids in proteins. *Proteins 56*, 102–109.
26. Brasseur, R. (1995) Simulating the folding of small proteins by use of the local minimum energy and the free solvation energy yields native-like structures. *J. Mol. Graphics 13*, 312–322.
27. Lins, L., Thomas, A., and Brasseur, R. (2003) Analysis of accessible surface of residues in proteins. *Protein Sci. 12*, 1406–1417.
28. Wei, X., Decker, J. M., Liu, H., Zhang, Z., Arani, R. B., Kilby, J. M., Saag, M. S., Wu, X., Shaw, G. M., and Kappes, J. C. (2002) Emergence of resistant human immunodeficiency virus type 1 in patients receiving fusion inhibitor (T-20) monotherapy. *Antimicrob. Agents Chemother. 46*, 1896–1905.
29. Epand, R. M. (2007) Detecting the presence of membrane domains using DSC. *Biophys. Chem. 126*, 197–200.
30. Vishwanathan, S. A., Thomas, A., Brasseur, R., Epand, R. F., Hunter, E., and Epand, R. M. (2008) Hydrophobic Substitutions in the First Residue of the CRAC Segment of the gp41 Protein of HIV. *Biochemistry 47*, 124–130.
31. Epand, R. M., Bach, D., Borochov, N., and Wachtel, E. (2000) Cholesterol crystalline polymorphism and the solubility of cholesterol in phosphatidylserine. *Biophys. J. 78*, 866–873.
32. Loomis, C. R., Shipley, G. G., and Small, D. M. (1979) The phase behavior of hydrated cholesterol. *J. Lipid Res. 20*, 525–535.
33. Aloia, R. C., Tian, H., and Jensen, F. C. (1993) Lipid composition and fluidity of the human immunodeficiency virus envelope and host cell plasma membranes. *Proc. Natl. Acad. Sci. U.S.A. 90*, 5181–5185.
34. Brugger, B., Glass, B., Haberkant, P., Leibrecht, I., Wieland, F. T., and Krausslich, H. G. (2006) The HIV lipidome: A raft with an unusual composition. *Proc. Natl. Acad. Sci. U.S.A. 103*, 2641–2646.
35. Leung, K., Kim, J. O., Ganesh, L., Kabat, J., Schwartz, O., and Nabel, G. J. (2008) HIV-1 assembly: Viral glycoproteins segregate quantally to lipid rafts that associate individually with HIV-1 capsids and virions. *Cell Host Microbe 3*, 285–292.
36. Luo, C., Wang, K., Liu, D. Q., Li, Y., and Zhao, Q. S. (2008) The functional roles of lipid rafts in T cell activation, immune diseases and HIV infection and prevention. *Cell. Mol. Immunol. 5*, 1–7.
37. Guyader, M., Kiyokawa, E., Abrami, L., Turelli, P., and Trono, D. (2002) Role for human immunodeficiency virus type 1 membrane cholesterol in viral internalization. *J. Virol. 76*, 10356–10364.
38. Zhu, P., Liu, J., Bess, J., Jr., Chertova, E., Lifson, J. D., Grise, H., Ofek, G. A., Taylor, K. A., and Roux, K. H. (2006) Distribution and three-dimensional structure of AIDS virus envelope spikes. *Nature 441*, 847–852.
39. Zanetti, G., Briggs, J. A., Grunewald, K., Sattentau, Q. J., and Fuller, S. D. (2006) Cryo-electron tomographic structure of an immunodeficiency virus envelope complex in situ. *PLoS Pathog. 2*, e83.

BI8014828